

RADIANT EXTINCTION OF GASEOUS DIFFUSION FLAMES

S. Berhan, M. Chernovsky and A. Atreya

Department of Mechanical Engineering, U of M; Ann Arbor, MI 48109

Howard R. Baum

BFRL, NIST; Gaithersburg, MD 20899

Kurt R. Sacksteder

NASA Glen Research Center; Cleveland, OH 44135

INTRODUCTION

The absence of buoyancy-induced flows in microgravity (μg) and the resulting increase in the reactant residence time significantly alters the fundamentals of many combustion processes. Substantial differences between normal gravity (ng) and μg flames have been reported in experiments on candle flames [1, 2], flame spread over solids [3, 4], droplet combustion [5,6], and others. These differences are more basic than just in the visible flame shape. Longer residence times and higher concentration of combustion products in the flame zone create a thermochemical environment that changes the flame chemistry and the heat and mass transfer processes. Processes such as flame radiation, that are often ignored in ng , become very important and sometimes even controlling. Furthermore, microgravity conditions considerably enhance flame radiation by: (i) the build-up of combustion products in the high-temperature reaction zone which increases the gas radiation, and (ii) longer residence times make conditions appropriate for substantial amounts of soot to form which is also responsible for radiative heat loss. Thus, it is anticipated that radiative heat loss may eventually extinguish the "weak" (low burning rate per unit flame area) μg diffusion flame. Yet, space shuttle experiments on candle flames show that in an infinite ambient atmosphere, the hemispherical candle flame in μg will burn indefinitely [1]. This may be because of the coupling between the fuel production rate and the flame via the heat-feedback mechanism for candle flames, flames over solids and fuel droplet flames. Thus, to focus only on the gas-phase phenomena leading to radiative extinction, aerodynamically stabilized gaseous diffusion flames are examined. This enables independent control of the fuel flow rate to help identify conditions under which radiative extinction occurs. Also, spherical geometry is chosen for the μg experiments and modeling because: (i) It reduces the complexity by making the problem one-dimensional. (ii) The spherical diffusion flame completely encloses the soot which is formed on the fuel rich side of the reaction zone. This increases the importance of flame radiation because now both soot and gaseous combustion products co-exist inside the high temperature spherical diffusion flame. (iii) For small fuel injection velocities, as is usually the case for a pyrolyzing solid, the diffusion flame in μg around the solid naturally develops spherical symmetry. Thus, spherical diffusion flames are of interest to fires in μg and identifying conditions that lead to radiation-induced extinction is important for spacecraft fire safety.

EXPERIMENTAL RESULTS

The experiments were conducted in the 2.2 sec drop tower at the NASA Glenn Research Center. The drop-rig used is described in detail elsewhere [7]. Briefly, it consists of a cylindrical test chamber (0.38m dia.; 0.43m deep) that houses the spherical burner, the hot-wire igniter and the photodiodes and thermocouples used for making radiation and temperature measurements. The spherical burner (19mm dia.) was constructed from a low heat capacity porous ceramic material (93% porosity). Two gas cylinders (150 cc & 500 cc) were charged with various gases up to 45 psig and were used to supply the fuel to the porous spherical burner. Fuel flow rates to the burner were controlled by a calibrated needle valve and a gas solenoid valve was used to open and close the gas line to the burner upon computer command. The test chamber also had a 125mm diameter Lexan

window which enabled the camera to photograph the flame.

Several μg experiments under ambient pressure and oxygen concentration conditions, were conducted with methane (less sooty), ethylene (sooty), and acetylene (very sooty) fuels for flow rates ranging from 3 to 45 cm^3/s . Only a few results are presented here. The data was collected by an onboard computer during the drop and the following measurements were made: (i) *Flame radius* – measured from photographs taken by a color CCD camera (see Figure 1 for three experiments on methane at different flow rates). (ii) *Flame radiation* – measured by photodiodes with different spectral characteristics ranging from UV to IR (See figures 2 & 3 for comparable flow rates of acetylene and methane. Here, the radiation emitted by the flame in different

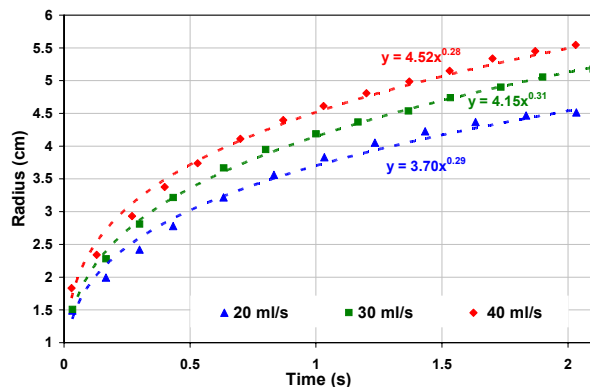


Figure 1: Methane Radius Measurements

evolution of radial temperature profiles is shown in Figure 4 for an acetylene flame.

Video photographs show that for all fuels (methane, ethylene and acetylene), initially the flame was blue (non-sooty) but becomes very bright yellow (sooty) under μg conditions. Later, as the μg time progresses, the flame grows in size and becomes orange and less luminous and the soot luminosity disappears. For the same fuel flow rate, methane flames eventually become blue (non-sooty) in approximately one second, ethylene flames became blue toward the end of the μg time (i.e. ≈ 2 sec) while acetylene flames remained luminous yellow throughout the 2.2 sec μg time. However, the luminosity of acetylene flames was considerably reduced toward the end of the μg time and would have also become blue given more time. These visual observations are in agreement with the flame radiation measurements shown in Figures 2 & 3 for C_2H_2 & CH_4 respectively. Radiation for CH_4 flames (Fig. 3) gradually increases and then decreases. This is true not just for the visible radiation but also for the infrared radiation containing the major CO_2 and H_2O bands. Clearly, the flame gases are cooling at a rate faster than the combustion heat release. Given sufficient time the flame is expected to extinguish. However, the situation is different for acetylene flames. First, the flame radiation is significantly larger due to soot formation

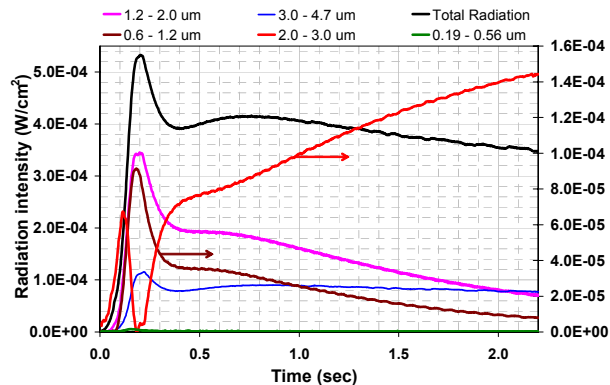


Figure 2: Acetylene 45 ml/s - Radiation Measurements

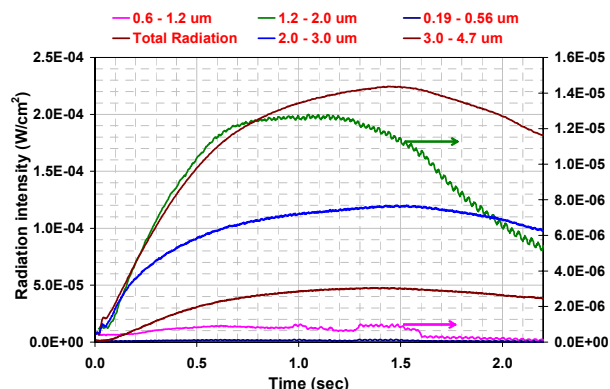


Figure 3: Methane 40 ml/s - Radiation Measurements

wavelength intervals is plotted). (iii) *Flame temperature* – measured by five S-type thermocouples and the sphere surface temperature was measured by a K-type thermocouple. The

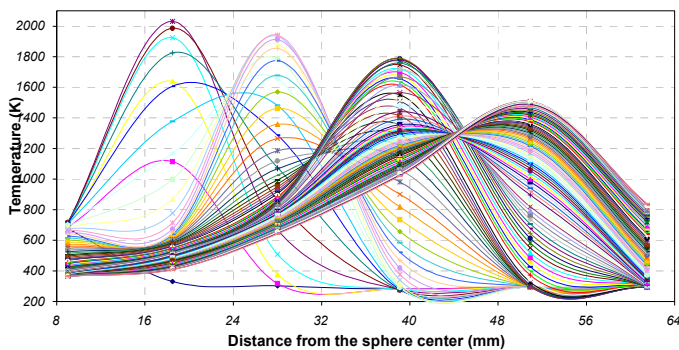


Figure 4: Evolution of radial temperature profiles - C_2H_2 (Drop 113 - 45 ml/s)

and oxidation in the vicinity of the high temperature reaction zone. This is responsible for the large rise and decrease in the first 0.4 seconds. As time proceeds, the radiation from all wavelengths decreases except radiation from the 2-3 μ m band which contains the combined CO₂ and H₂O bands. The 3-4.7 band, corresponding to CO₂, however, stays constant but shows a slight peak for t<0.4sec. Since the combined CO₂ & H₂O band dips considerably in this zone, it implies that the increase in radiation is primarily due to soot oxidation. Later, as the distance between the soot shell and the reaction zone increases, only H₂-rich species are burning resulting in an increase in the H₂O band radiation. It would be interesting to calculate the H₂, H₂O and CO₂ CO and OH profiles in this region. Figure 4 provides the radial temperature distribution corresponding to Figure 2. Clearly, the flame temperature continuously falls and we expect even acetylene flame to extinguish given sufficient time.

THEORETICAL RESULTS

To better understand these processes and predict flame radius, radiation and temperature, theoretical models are being developed with chemical kinetics and flame radiation. As a first step, soot formation and oxidation is not included and three types of models are considered: (i) Assuming infinite reaction rate (analytical), (ii) Assuming a single-step reaction mechanism, and (iii) Using a skeletal reaction mechanism from Smooke[10]. Also, emission approximation was made in all cases for modeling the flame radiation. For the simplest case of *constant pressure ideal gas reactions*, we may write the following governing equations for an approximate analysis under conditions of small soot loading:

$$\text{Mass Conservation : } \frac{\partial \rho}{\partial t} + \frac{1}{r^2} \frac{\partial}{\partial r} (r^2 \rho v) = 0 \quad (1)$$

$$\text{Conserved Scalar : } \rho \frac{\partial Z}{\partial t} + \rho v \frac{\partial Z}{\partial r} - \frac{1}{r^2} \frac{\partial}{\partial r} \left(r^2 \rho D \frac{\partial Z}{\partial r} \right) = 0 \quad (2)$$

$$\text{Constant Pressure Ideal gas : } \rho T = \rho_{\infty} T_{\infty} \text{ or } \rho h^s = \text{const.} \quad (3)$$

$$\text{Defining : } \frac{\partial \psi}{\partial t} = - r^2 \rho v ; \frac{\partial \psi}{\partial r} = r^2 \rho ; \Rightarrow \left(\frac{\partial r}{\partial t} \right)_{\psi} = v \quad (4)$$

Here, the symbols have their usual definitions with ρ = density, T = temperature, v = velocity, Z = Conserved Scalar (mixture fraction variable), h^s = sensible enthalpy and D = diffusion coefficient. Species and energy equations are replaced by a mixture fraction variable 'Z' which is described by a homogeneous equation. The expectation is that this approach may be adequate for calculating the observed expansion rate of the spherical diffusion flames, but it is expected to be inadequate for predicting radiative extinction.

Applying the corresponding initial and boundary conditions for a sphere of radius 'R' blowing fuel gases at a rate $\dot{M}(t)$ we get:

$$\psi(r, t) = \int_{R(t=0)}^{r(t)} r^{*2} \rho (r^*, t) dr^* - \frac{M(t)}{4\pi} \quad (5)$$

Where $M(t)$ is the total fuel mass that has been injected from the sphere in time 't'. For a constant given mass injection rate $\dot{M}(t)$, $M(t) = \dot{M}(t) \times t$. Using $\psi = \psi_o = \text{const}$ at $r = r_f$ we obtain in the approximation $Z = Z_c$:

$$r_f(t) = \left(R^3 + \left(\frac{3\dot{V} (\rho_o h_{\infty}^s + Q \rho_o Y F_{\infty} Z_c)}{4\pi (\rho_o h_{\infty}^s + \bar{\eta} t)} \right) \times t \right)^{1/3} \quad (6)$$

Where, $\bar{\eta}$ = Average heat loss rate by radiation per unit volume. Data correlated according to equation (6) is shown in Figure 5. Clearly, while Equ (6) is approximate, it captures the physics of flame growth. The fact that most of the data falls along a constant value (~ 1.3) is very encouraging. Furthermore, the numerical calculations with one step reaction mechanism and thin gas radiation also falls along this constant value. Numerical calculations without radiation clearly do not agree with the data. Figures 6 & 7 show calculations with a detailed mechanism. Note how the OH mass fraction and temperature are reduced at extinction.

Acknowledgements: This project was supported by NASA under the Contract No.: NCC3-482.

REFERENCES

1. Dietrich, D. L., Ross, H. D. and T'ien, J. S. "Candle Flames in Microgravity," Third Microgravity Combustion Workshop, Cleveland, Ohio, April, 1995.
2. Ross, H. D., Sotos, R. G. and T'ien, J. S., Combustion Science and Technology, Vol. 75, pp.155-160, 1991.
3. T'ien, J. S., Sacksteder, K. R., Ferkul, P. V. and Grayson, G. D. "Combustion of Solid Fuels in very Low Speed Oxygen Streams," Second International Microgravity Combustion Workshop," NASA Conference Publication, 1992.
4. Ferkul, P., V., "A Model of Concurrent Flow Flame Spread Over a Thin Solid Fuel," NASA Contractor Report 191111, 1993.
5. Jackson, G., S., Avedisian, C., T. and Yang, J., C., Int. J. Heat Mass Transfer., Vol.35, No. 8, pp. 2017-2033, 1992.
6. Tsue, M., Segawa, D., Kadota, T. and Yamasaki, H. Twenty-Sixth (International) Symposium on Combustion, The Combustion Institute, 1996, pp. 1251-1258.
7. Atreya, A, Agrawal, S., Sacksteder, K., and Baum, H., "Observations of Methane and Ethylene Diffusion Flames Stabilized around a Blowing Porous Sphere in g Conditions," AIAA # 94-0572.
8. Zhang, C., Atreya, A. and Lee, K., Twenty-Fourth (International) Symposium on Combustion, The Combustion Institute, pp. 1049-1057, 1992.
9. Atreya, A. and Agrawal, S., "Effect of Radiative Heat Loss on Diffusion Flames in Quiescent Microgravity Atmosphere," *Combustion & Flame*, p372-382, v115, 1998.
10. Smooke, M. D.(ed.) "Reduced Kinetic Mechanisms and Asymptotic Approximations for Methane-Air Flames," Springer-Verlag, 1991.

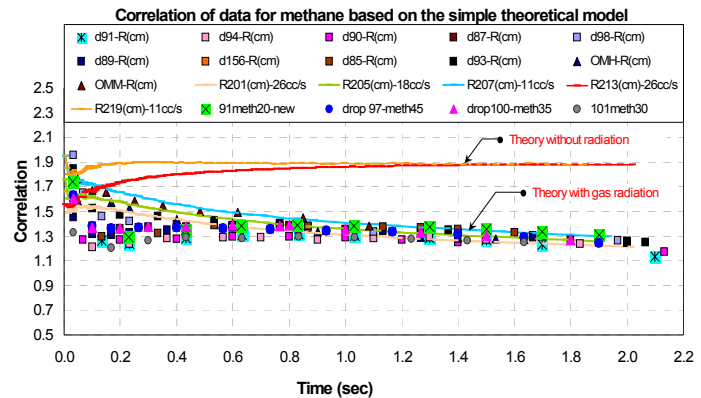


Figure 5

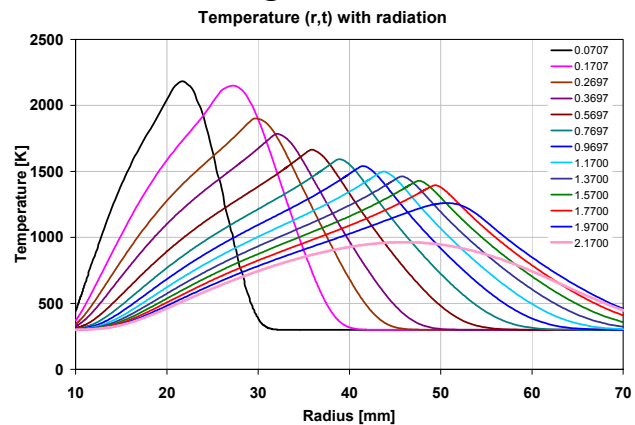


Figure 6: Decrease in the flame temperature due to radiation – Smooke's mechanism [10]

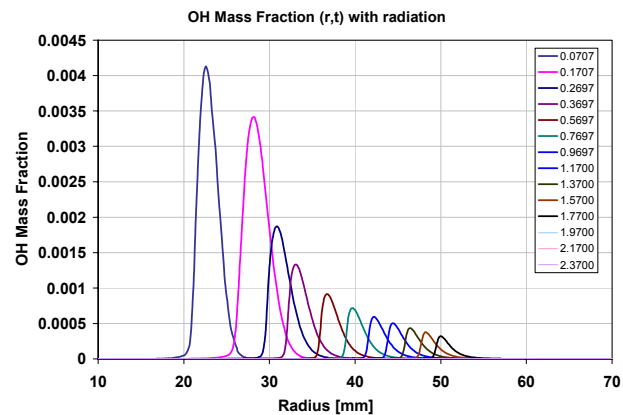


Figure 7: Decrease on OH mass fraction as the flame tends towards extinction.